

A SIMPLE ANALYTICAL MODEL FOR THE DESIGN OF VERTICAL TUBE ABSORBERS

V. Patnaik

H. Perez-Blanco, Ph.D.
Associate Member ASHRAE

W.A. Ryan

ABSTRACT

The absorption of water vapor in aqueous solutions of lithium bromide is modeled for a falling-film, vertical-tube absorber. The model is based on the solution of three ordinary differential equations to calculate axial solution concentration and temperature distributions and coolant temperature distribution. The heat and mass transfer coefficients employed in the equations are extracted from the literature, incorporating recent information on wavy-laminar flows. Under certain conditions, the numerical solution exhibits instabilities in the entrance region of the absorber tube, which are corrected by the introduction of a dampening factor incorporating relevant thermophysical properties. The usefulness of the model for generating absorber performance charts is demonstrated.

INTRODUCTION

In absorption machines employed for heating and cooling applications (Stoecker and Jones 1982), simultaneous heat and mass transfer operations take place in the absorber and generator. Present understanding of the transfer operations in falling-film absorbers is incomplete, leading to design approaches that are largely empirical and confined to smooth-tube absorbers only. It is customary to employ an empirical heat transfer coefficient and assume that it adequately reflects the combined heat and mass transfer process. This approach is only valid in calculations for similar absorbers and at similar operating conditions. For new absorber types or for different operating conditions, design tools do not exist.

Previous work has developed an understanding of the transport processes in both laminar and turbulent absorber falling films. The energy and diffusion equations were solved by Grossman (1983) for laminar films for both isothermal and adiabatic walls. Charts for calculation of the film's Nusselt and Sherwood numbers, as a function of normalized absorber length, were produced. Laminar falling films over adiabatic walls were also studied in Goff et al. (1985), which contains information on the effectiveness of heat and mass transfer to the falling film. A simple model for absorption of vapors into falling films was described in Andberg and Vliet (1983), based on the assumed similarity of the concentration profiles. Comparison of model predictions to experimental results showed good agreement. Nonisothermal absorption in wavy-transition and turbulent

films was characterized experimentally in Yueksel and Schluender (1988), and comparisons to theoretical predictions were made, yielding agreement on the order of 30% for mass transfer coefficients. More recently, experimental work was also done by Cosenza and Vliet (1990), who provided a heat transfer correlation for the film absorption process on horizontal tubes.

Empirical design approaches, most of them unpublished, exist for horizontal tube bundles. Vertical tube absorbers have been used for small residential and large industrial absorption machine prototypes. When reduced footprints are desired, or when multistaging calls for falling films on both sides of a vertical surface, vertical tube absorbers may be required. A vertical tube absorber model yields insights into the transport processes within falling films, also occurring in horizontal tube absorbers.

A persistent problem in absorber design is that earlier theoretical information applies to laminar, rather than wavy-laminar, films. Wavy flow arises even at low Reynolds numbers (Perez-Blanco 1988). Consequently, design approaches based on laminar flow theory tend to underpredict the mass transport to the film (Perez-Blanco 1988; Grossman 1984), hence the absorber capacity. There is a conflict over the reasons for the enhancement and its magnitude. According to Grossman (1984), theories based on the inclusion of the transverse velocity component in the model yield better agreement with experiments than the theories based on the Levich surface-tension models. Further evidence supporting the importance of the normal velocity component is given in McCready and Hanratty (1984), where it is shown that both low- and high-frequency velocity components can result in concentration fluctuations that influence mass transport at a clean gas-liquid interface.

Consequently, a design approach is required that can accurately reflect the energy and species transport operations. For instance, if the coolant flow is changed, the heat transfer coefficient will vary. However, if the absorber capacity is limited by the mass transfer rate instead of the coolant heat transfer coefficient, changes in capacity may be minimal and will not completely reflect the change in heat transfer coefficients. The ultimate target of our work is to develop a simple design tool that can be used to design new absorbers with both smooth and advanced tube surfaces (Patnaik et al. 1992).

In this work, we present a vertical-tube lithium bromide absorber model incorporating recent empirical information on wavy-laminar and wavy-transitional films (Yih and Chen

Vikas Patnaik is a graduate research assistant and Horacio Perez-Blanco is an associate professor in the Department of Mechanical Engineering, Pennsylvania State University, University Park. William A. Ryan is with the Gas Research Institute, Chicago, IL.

1982). The practical possibilities offered by the model are shown in the results section, which contains information summarized in a graphical form to facilitate absorber design.

MODEL DESCRIPTION

A schematic diagram of the falling-film, vertical-tube absorber is shown in Figure 1. Countercurrent coolant and absorbent solution flow is considered, as indicated in the figure. The coolant is water, and the absorbent solution is an aqueous solution of lithium bromide. The solution flows as a falling film on the outer surface of the absorber tube, entering concentrated at the top and leaving diluted at the bottom of the tube after absorbing water vapor. The heat of absorption, coupled with the heat transfer between the solution and the cooling water, results in axial temperature variations in both fluids. Numerical solution of the governing equations for this coupled heat and mass transfer problem then yields the temperatures and solution concentration distributions, based on the following assumptions:

1. steady-state conditions, and
2. a one-dimensional problem: only variation of flow properties in the axial direction is of interest.

The following magnitudes are assumed to be constant:

3. the specific heat of both coolant and absorbent solution;
4. other thermophysical properties of the coolant (since its temperature stays nearly constant);
5. the heat transfer coefficient on the coolant side of the tube, owing to fully developed velocity and temperature profiles; and
6. the heat of absorption.

In addition,

7. the falling film is laminar or wavy-laminar;
8. vapor pressure equilibrium exists at the vapor-solution interface;
9. the bulk solution temperature profile is linear with respect to the transverse coordinate;
10. the vapor is still, with uniform pressure (which is the absorber pressure) and temperature;
11. the vapor-side resistance to mass transfer is negligible, i.e., there are no noncondensibles in the vapor phase;
12. the vapor drag on the falling film is negligible;
13. the heat transferred from the solution to the vapor is negligible; and
14. the vapor mass absorbed is very small compared to solution flow, as established by empirical studies.

The Governing Equations

The theoretical model is constructed from two energy balances and a mass balance on an infinitesimally thin slice of the absorber tube (see appendix). These balances yield three independent equations in the three dependent vari-

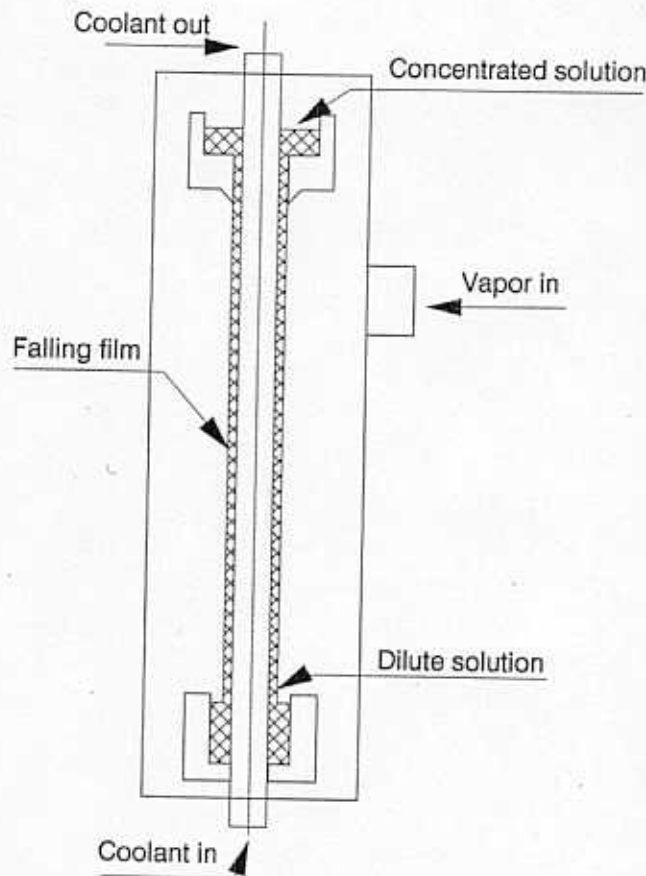


Figure 1 Schematic of a falling film absorber.

ables—coolant temperature, solution (bulk) temperature, and solution mass flow rate—and the independent variable—vertical distance from the top of the absorber tube. Thus we have, after nondimensionalization with respect to the coolant outlet properties (T_{co} , m_c , c_{pc}),

$$\frac{dT_s^*}{dz^*} = -\frac{1}{M_s^*} \left[\frac{dm_s^*}{dz^*} (H_v^* - c_{ps}^* T_s^*) + U^* \{ 1 - T_s^* (1 - M_s^*) - H_v^* (m_s^* - m_{s1}^*) - M_{s1}^* T_{s1}^* \} \right], \quad (1)$$

where dm_s^*/dz^* is obtained as the second first-order ordinary differential equation (ODE),

$$\frac{dm_s^*}{dz^*} = \frac{2\pi r_o L}{m_c} \cdot \frac{Sh D_{AB}}{\delta} \cdot \rho_s (x_s - x_{if}), \quad (2)$$

the film thickness being given by

$$\delta = \left(\frac{3 \cdot \mu \cdot \Gamma}{\rho^2 \cdot g} \right)^{\frac{1}{3}}, \quad (3)$$

as obtained from Nusselt's classic solution (Seban 1978), which also yields the film velocity profile. The third ODE relates to the coolant temperature:

$$\frac{dT_c^*}{dz^*} = -U^*(T_s^* - T_c^*). \quad (4)$$

Interface and Inlet Conditions

To calculate the liquid interface temperature, an energy balance on an infinitesimally thin control volume of length dz enclosing the interface is performed (see appendix). Based on a linear temperature profile in the film (assumption 9), we obtain

$$T_{if}^* = T_s^* + \frac{M_c H_v^*}{8\pi L k_s} \cdot \frac{\delta}{r_o + \delta} \cdot \frac{dm_s^*}{dz^*}. \quad (5)$$

Using this interface temperature and the known absorber pressure, p_v , we obtain the interface solution concentration from the property values of lithium bromide-water solutions as

$$x_{if} = f(T_{if}, p_v). \quad (6)$$

Equations 5 and 6 can be interpreted as conditions at the vapor-liquid interface. The coolant and LiBr-solution conditions at their respective entrances constitute the inlet conditions for the mathematical model described above:

$$\begin{aligned} z^* = 0, \quad T_s^* &= T_{if}^* = T_{s_i}^*, \\ x_s &= x_{if} = x_{s_i}, \\ m_s^* &= m_{s_i}^* \end{aligned} \quad (7)$$

$$z^* = 1, \quad T_c^* = T_{c_i}^*. \quad (8)$$

Solution Method

The three governing equations form a dimensionless system of nonlinear, first-order ordinary differential equations. A fourth-order Runge-Kutta scheme is used to perform the numerical integration of the above coupled differential equations (Davis and Polonsky 1970). The integration proceeds from $z^* = 0$ to $z^* = 1$ under an assumed value for the exit coolant temperature. If the computed inlet temperature does not match the given value within the chosen convergence criterion of $O(10^{-7})$, the initial guess is improved using a bisection technique, and the "downward march" is repeated until convergence is attained (Carnahan et al. 1969).

The Dampening Factor

When the inlet conditions reflect superheating of the aqueous solution, numerical instabilities arise in the computed interface temperature and concentration in the entrance region, i.e., 0.3% of the tube length (Figure 2).

To remove the oscillatory behavior, a *dampening factor* was introduced in the boundary condition at the vapor-liquid interface (Equation 5) analogous to first-order step-response theory in electrical measurements (Close and Frederick 1978). This factor is an increasing function of time (asymptotically approaching unity) having the form:

$$R = 1 - e^{-\frac{z\alpha_s}{v_{max}\delta^2}}. \quad (9)$$

Inserting this factor in Equation 5, the dampened interface solution temperature becomes

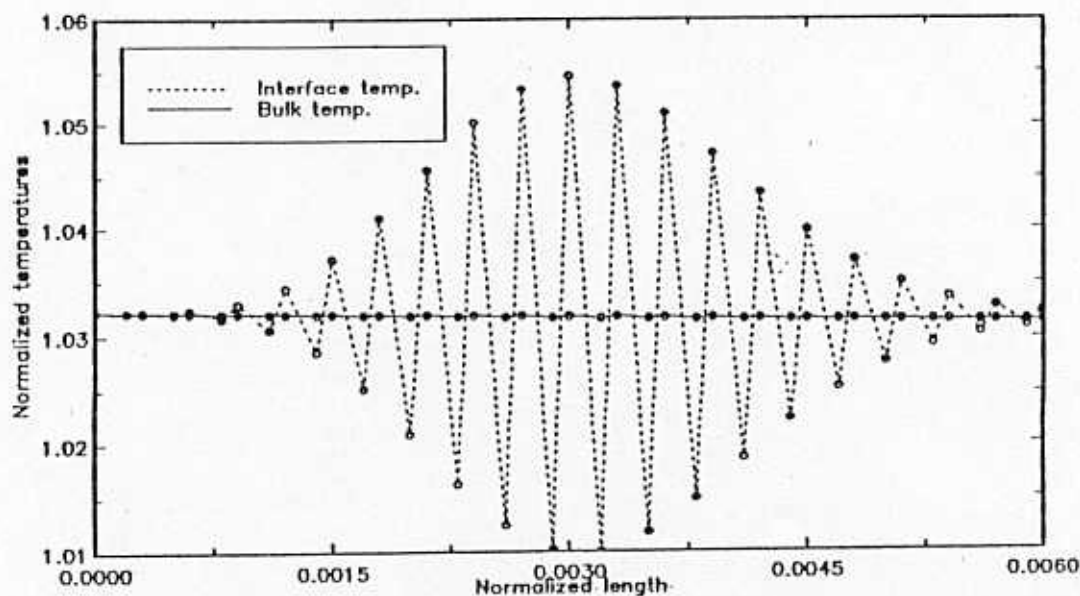


Figure 2 Instability in the entrance region.

$$T_{if}^* = T_s^* + R \cdot \frac{M_c H_v^*}{8 \pi L k_s} \cdot \frac{\delta}{r_o + \delta} \cdot \frac{dm_s^*}{dz^*} \quad (10)$$

The introduction of the dampening factor thus resolves the problem of instability near the upper entrance without affecting the temperature and concentration variations further downstream. This is illustrated in Figure 3, in comparison with Figure 2.

HEAT AND MASS TRANSFER COEFFICIENTS

Values for the heat and mass transfer coefficients are required to solve the given problem.

Overall Heat Transfer Coefficient

The overall heat transfer coefficient is obtained as the inverse of the result of three resistances: convective resistances on the coolant and falling-film sides and the conductive resistance of the tube wall. Fouling factors can be included. Thus, we have

$$U = \left(\frac{r_o}{r_{in}} \frac{1}{h_c} + \frac{r_o}{k_w} \ln \frac{r_o}{r_{in}} + \frac{1}{h_s} \right)^{-1} \quad (11)$$

The correlations for the coolant and film heat transfer coefficients used by the model are as follows:

Fully developed coolant flow through tube or annulus:

Laminar: Incropera and DeWitt (1990) (valid for isothermal wall).

Turbulent: Gnielinski's correlation (valid for both isothermal wall and constant heat flux wall) (Kays and Perkins 1985),

$$Nu_c = \frac{(Re_{D_h} - 1000) Pr_c \cdot f/2}{1.0 + 12.7 (Pr_c^{2/3} - 1) \sqrt{f/2}}$$

$$2300 \leq Re_{D_h} < 5 \times 10^6, \quad 0.5 < Pr_c < 2000$$

using Petukhov's friction coefficient (Kays and Perkins 1985),

$$f = [1.58 \ln(Re_{D_h}) - 3.28]^{-2}$$

Falling film:

Thermal entrance region: Correlation due to Bays McAdams (intermediate between isothermal wall constant heat flux wall) (Knudsen 1973),

$$h_s = 1.29 \left(\frac{k_s^2 \rho_s^{4/3} c_{p,s}}{z \mu_s} \right)^{1/3} \cdot Re_s^{1/9}$$

Fully developed, wavy-laminar regime: Wilke's correlation (valid for constant heat flux wall, with progressive decreasing difference from isothermal wall outside entrance region) (Seban 1978),

$$\frac{h_s \delta}{k_s} = 0.029 (4 Re_s)^{0.53} Pr_s^{0.344}$$

The resistances to heat transfer were calculated for typical fully developed coolant and solution flows, results of which appear in Table 1.

The solution-side resistance is large compared to other components of the total thermal resistance. For high coolant flows, the tube wall resistance exceeds the coolant side resistance.

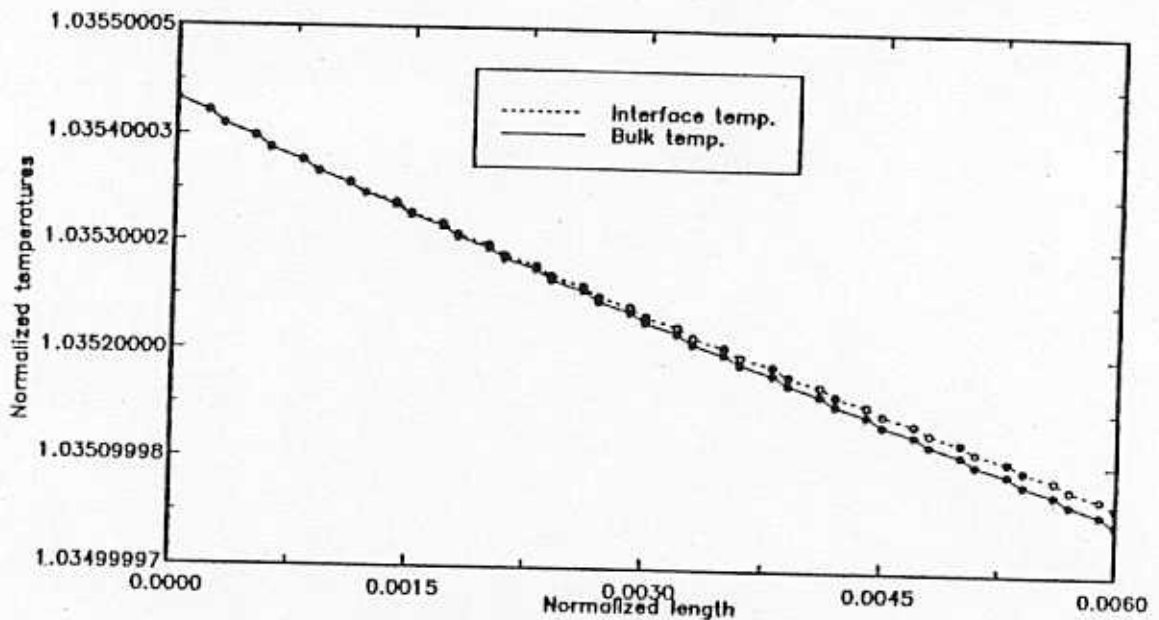


Figure 3 Instability eliminated with dampening factor.

TABLE 1
Representative Values of Thermal Resistances in Counterflow Coolant-Film System
($D_o = 19.05$ mm, $D_i = 10.32$ mm, $D_{ms} = 6.35$ mm, $L = 1.524$ m, tube material: SS 304L)

m_c [kg/s]	m_{si} [kg/s]	$r_o/(r_i \cdot h_c)$ [m ² ·K/W]	$r_o/k_w \cdot \ln(r_o/r_i)$ [m ² ·K/W]	$1/h_s$ [m ² ·K/W]	$1/U$ [m ² ·K/W]
0.025	0.010	0.000763	0.000392	0.000989	0.002143
0.050	0.015	0.000331	0.000392	0.000926	0.001650
0.100	0.020	0.000169	0.000392	0.000880	0.001441
0.200	0.020	0.000091	0.000392	0.000884	0.001367

Falling-Film Mass Transfer Coefficient

In the entrance region, the effect of interfacial waves on mass transport can be considered insignificant due to short exposure times, so that here Higbie's penetration theory (Hobler 1966) should be valid to yield:

$$\frac{\kappa_x \delta}{D_{AB}} = 1.38 \left(\frac{z}{\delta} \frac{1}{Re_x} \frac{1}{Sc_x} \right)^{-1/2} \quad (17)$$

This is combined with the asymptotic correlations of Yih and Chen (1982), based on a mass transfer mechanism associated with eddy dissipation at the surface:

$$\frac{\kappa_x \delta_r}{D_{AB}} = 1.099 \times 10^{-2} \cdot (4 Re_x)^{0.3955} Sc_x^{0.5}, \quad Re_x \leq 75 \quad (18)$$

$$\frac{\kappa_x \delta_r}{D_{AB}} = 2.995 \times 10^{-2} \cdot (4 Re_x)^{0.2134} \cdot Sc_x^{0.5}, \quad 75 < Re_x \leq 400 \quad (19)$$

where the reduced film thickness is given by

$$\delta_r = \left(\frac{v^2}{g} \right)^{1/3} \quad (20)$$

The maximum deviation between estimated prediction and actual values in such composite correlations usually occurs at the intersection of the curves (Seban 1978).

RESULTS AND DISCUSSION

The profiles of temperature versus distance from the top of the tube for the absorbent and coolant, obtained for a typical case, are shown in Figure 4. The interface temperature is greater than the bulk solution temperature, whereas the coolant temperature increases as it receives heat from the solution. Concentration variation with distance from the top, for the same case, is shown in Figure 5. While the interface LiBr concentration drops rapidly with absorption length, the bulk concentration decreases slowly. Thus, the rate of diffusion of water vapor limits transport into the falling film.

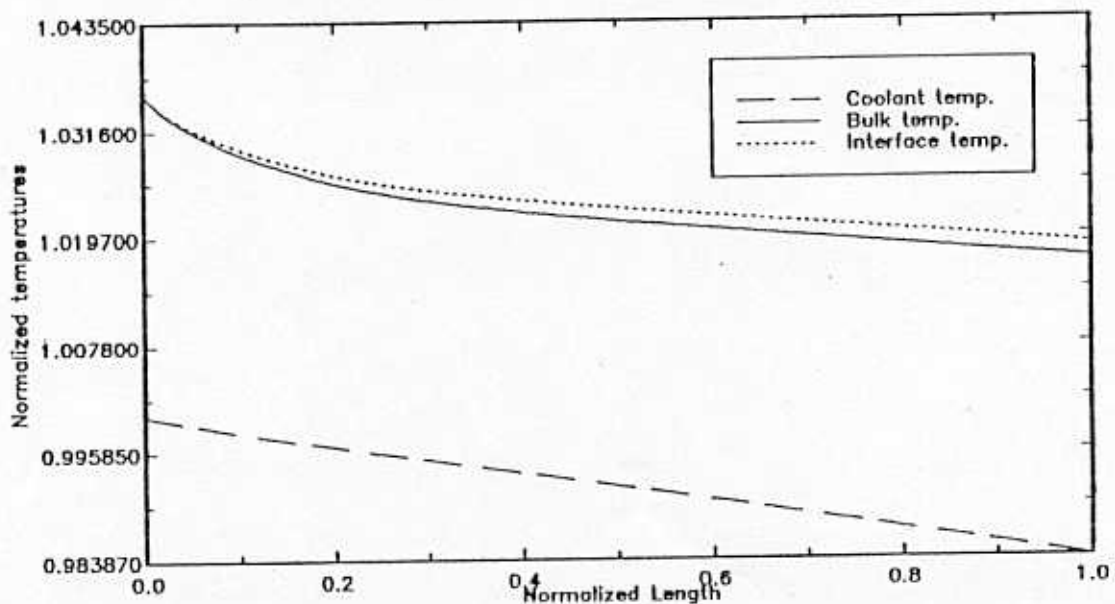


Figure 4 Typical solution, interface, and coolant temperature profiles.

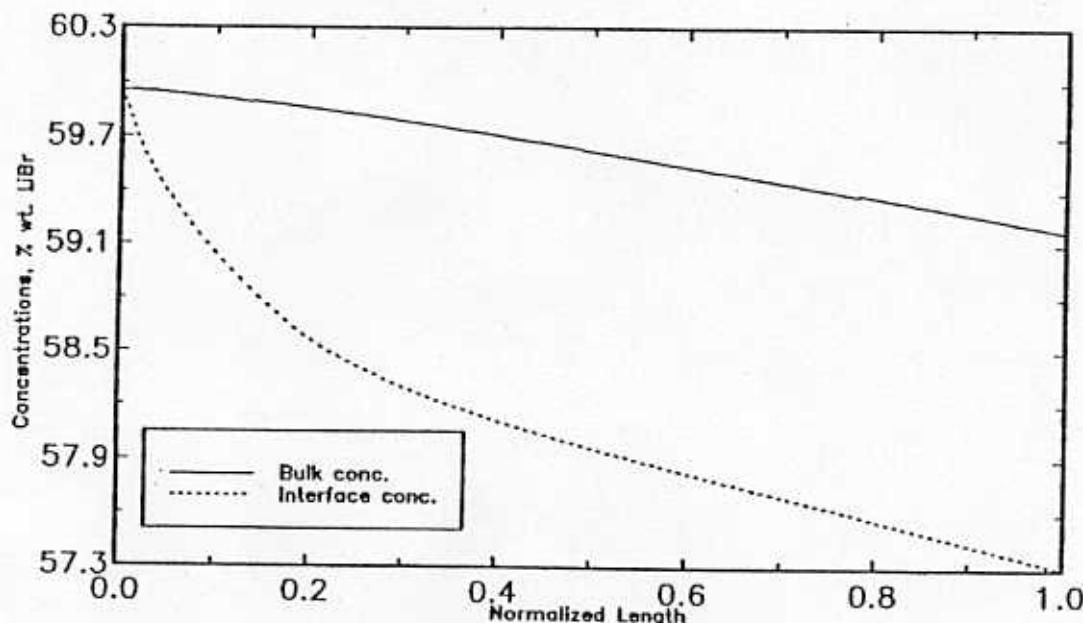


Figure 5 Typical solution bulk and interface concentration profiles.

The primary function of the absorber is to combine as much refrigerant as possible with the absorbent solution while also rejecting heat. The absorber heat load and mass absorbed are then important variables. The charts presented in Figures 6 and 7 thus give insight into the operational mode of the vertical-tube absorber. In these figures, the solution Reynolds numbers range from 155 to 311 and the coolant Reynolds numbers range from 3,973 to 31,785.

The mass absorbed (Figure 6) and the heat load (Figure 7) depend on tube length and on the coolant and solution flow rates. Both the mass absorbed and the heat load increase with the flow rates. However, at low coolant flows, the solution flow rate does not greatly influence the mass absorption rate. This is demonstrated in Figure 6, where, for a coolant rate of 0.025 kg/s, the mass absorbed is independent of solution flow rate. Since the latent heat load is practically the same for all the solution flow rates, only sensible heat load variation is reflected in Figure 7 (for $m_c = 0.025$ kg/s), wherein a doubling solution flow rate increases the sensible heat load by about 20%. The increase in sensible heat load is due to the increase in solution temperature since the overall heat transfer coefficient remains nearly constant. This constancy can be verified from Table 1, noting that the solution-side thermal resistance does not change significantly with solution flow rate. Thus, the solution temperature is higher for higher solution flow rates and, since the interface temperature will also be higher, the absorption rate should be reduced. The potential decrease in the mass absorbed due to a high interface temperature is compensated by an increase in the mass transfer coefficient with solution flow rate in such a way that the mass absorbed is nearly the same for all cases with the low coolant rate of 0.025 kg/s.

At higher coolant rates, the combined resistance to heat transfer in the coolant and wall is not quite as significant as for $m_c = 0.025$ kg/s (Table 1). The resulting effects of the solution and coolant flow rates on absorption are reflected clearly in Figures 6 and 7.

The solution exit concentration and exit temperature are shown in Figures 8 and 9. The exit brine concentration decreases with increasing coolant rates for all solution flow rates and tube lengths, as does the exit temperature. The exit concentration and temperature characterize the lack of equilibrium between the solution and vapor in the absorber. This lack of equilibrium is often expressed by means of a temperature difference, the "subcooling," which is defined as the difference between the temperature that the solution would have at the actual concentration and absorber pressure and the actual solution temperature.

For the cases considered here, the subcooling is zero at the absorber inlet. It would also be zero at the outlet of a tube of infinite length. This implies that the subcooling presents a maximum between the inlet and the outlet, which is evident in Figure 10. Subcooling is the parameter employed by many refrigeration engineers to gauge the effectiveness of an absorber, a minimal subcooling (with a given absorption area) being the design goal. It is interesting to note that the mass absorbed in Figure 6 and the subcooling displayed in Figure 10 correlate in that, for a given coolant flow, the subcooling increases and the mass absorbed decreases as the solution flow rate decreases. Thus, the evaporator capacity and the subcooling are related inversely to each other.

When heat/mass transfer additives are present, subcooling is small (on the order of a few degrees centigrade). This is the case in most horizontal-tube absorbers. For vertical-

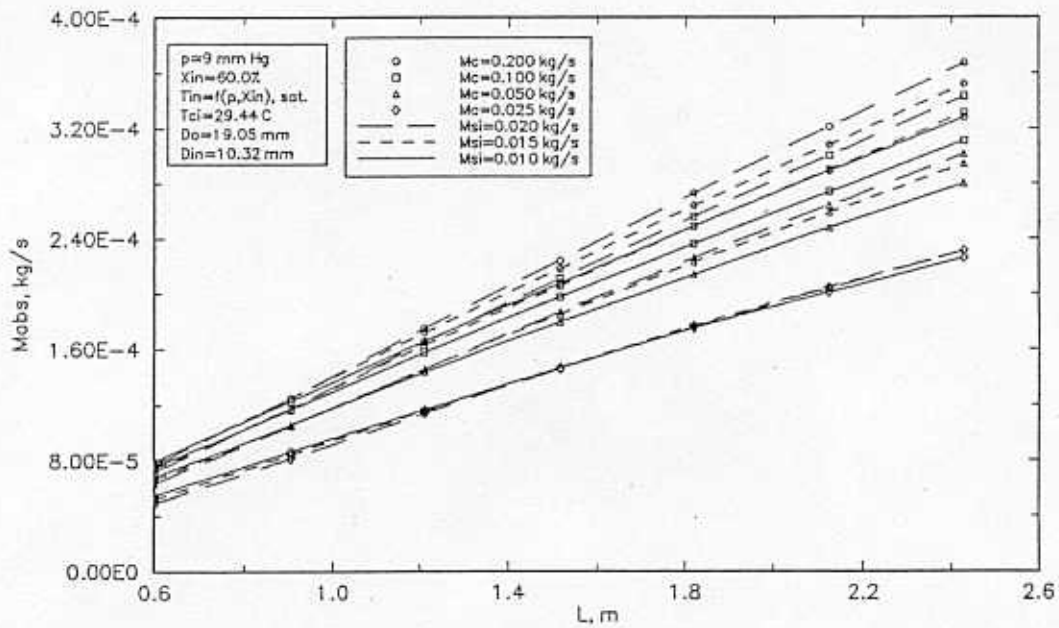


Figure 6 Performance chart for smooth vertical-tube absorbers: mass absorbed vs. absorber length.

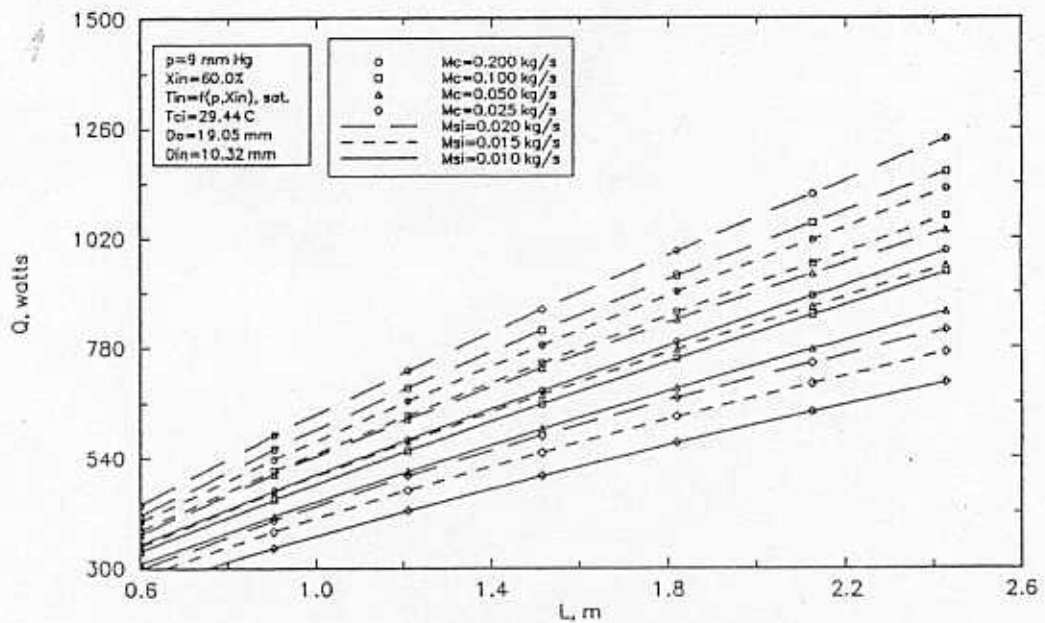


Figure 7 Performance chart for smooth vertical-tube absorbers: heat load vs. absorber length.

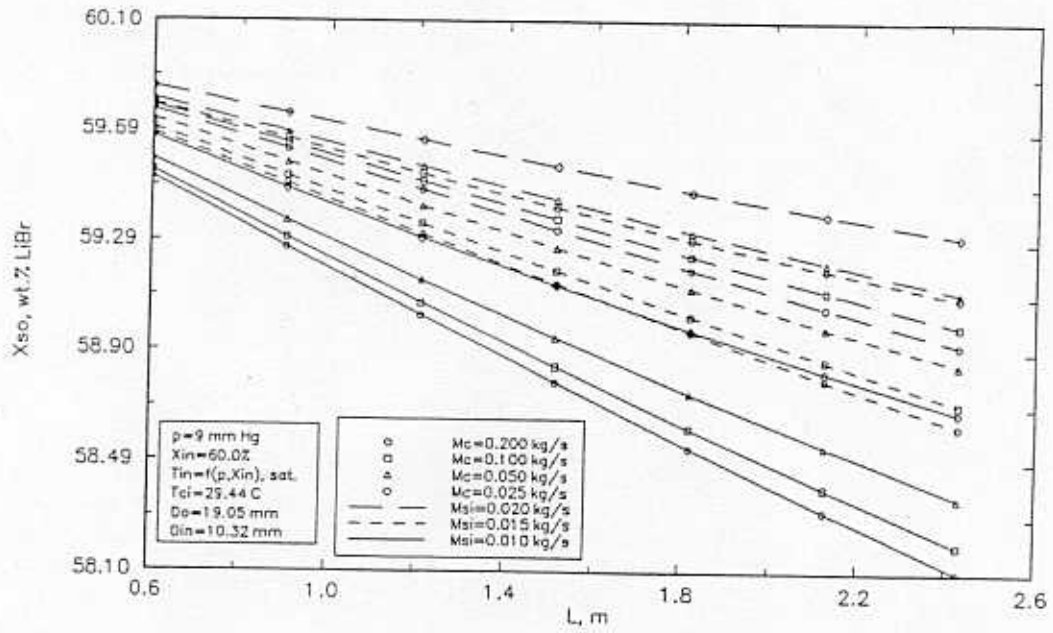


Figure 8 Performance chart for smooth vertical-tube absorbers: exit solution concentration vs. absorber length.

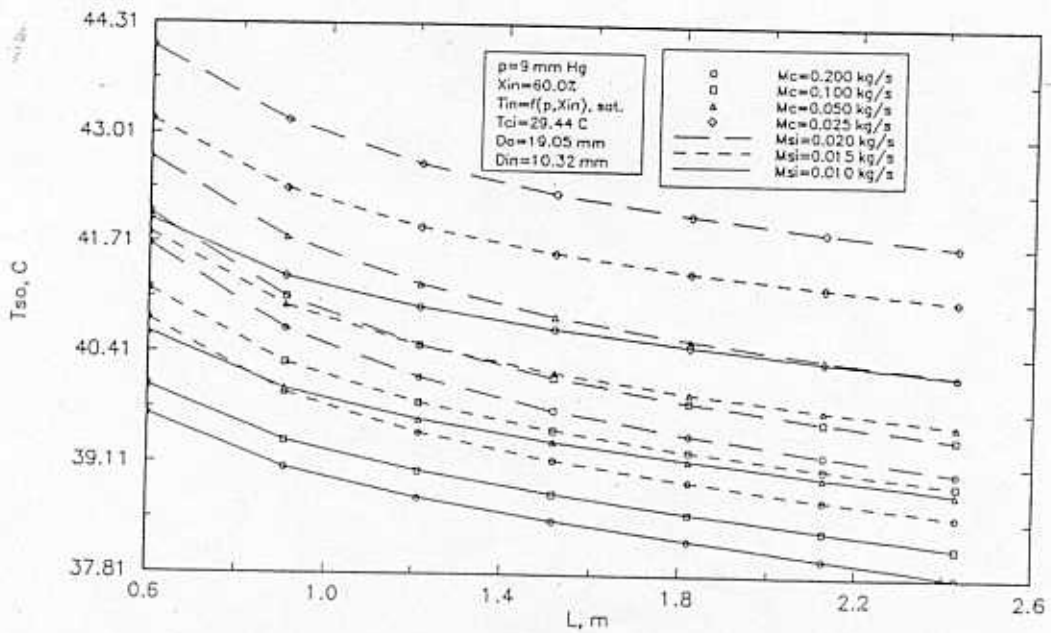


Figure 9 Performance chart for smooth vertical-tube absorbers: exit solution temperature vs. absorber length.

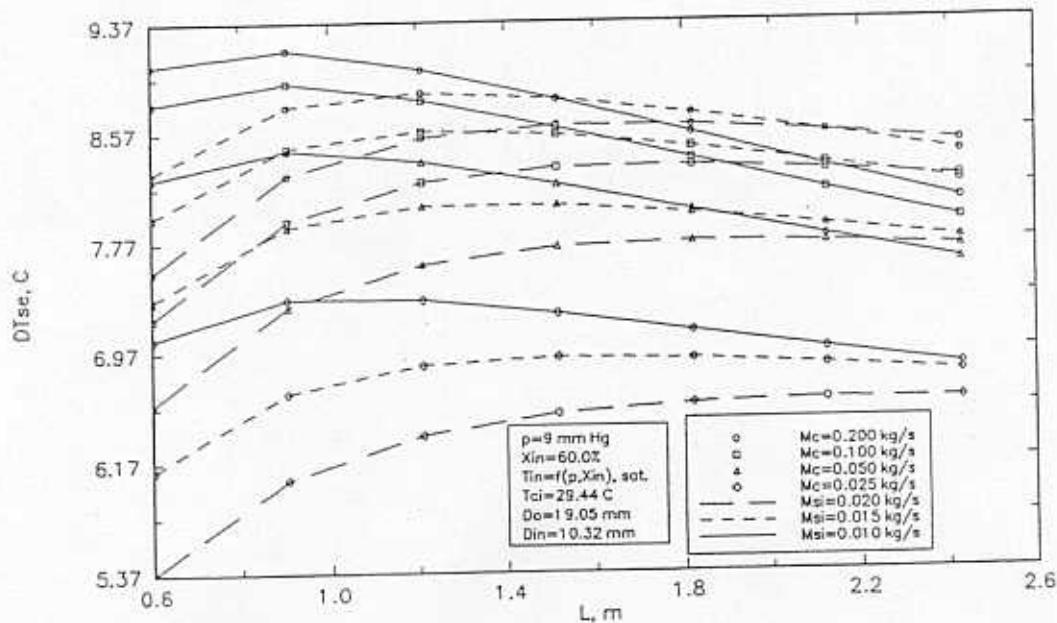


Figure 10 Performance chart for smooth vertical-tube absorbers: exit degree of subcooling vs. absorber length.

tube absorbers with no additives, the subcooling is indeed large (Figure 10). Additives in the falling film would result in an increased mass transfer coefficient, thereby reducing the subcooling.

Since no inerts were assumed to be present (assumption 11), the subcooling in this work is due to lack of equilibrium within the falling film. However, the net effect of the presence of inerts could readily be accounted for by modifying the model with the introduction of a resistance to mass transfer on the vapor side. In addition, reductions in the refrigerant vapor pressure due to the inerts would decrease the driving force for mass transfer.

In horizontal- and vertical-tube absorbers, noncondensibles increase the degree of subcooling. Depending on the absorber flow characteristics and the concentration of the inerts, the controlling mass transfer resistance could occur in the liquid or the vapor phase. In practice, the noncondensibles generated by corrosion or by minute leaks can build up to the point of seriously hampering machine performance.

CONCLUSION

A computational model of the vertical single-tube absorber using aqueous lithium bromide has been developed. The model can handle a wide range of operating conditions including superheated, equilibrium, or subcooled inlet conditions. Recent empirical correlations for the heat and mass transfer coefficients have been incorporated, which account for the wavy flow present in such falling-film absorbers.

The output of the model has been reduced to design charts based on a given set of operating parameters. The figures are performance maps of a smooth, vertical-tube absorber. The heat and mass transfer coefficients employed are extracted from empirical data in the literature. As long as the absorber flow regimes are consistent with those of the correlations, the maps should be accurate. The presence of mass transfer additives in the absorber will result in higher values for the mass transfer coefficient. Maps could also be generated for absorption with these additives if empirical data or accurate estimates on the enhanced mass transfer coefficient become available. However, the complete model must be validated against actual absorber experimental data, an ongoing activity (Patnaik et al. 1992).

The charts allow determination of absorber size and operating exit conditions for a given evaporator load. Thus, if the evaporator load is known and the coolant and solution flow rates are selected, the performance map will yield tube length (Figure 6) and heat load (Figure 7). The exit solution concentration, temperature, and degree of subcooling can also be read from the charts (Figures 8 through 10) for the obtained absorber length.

The charts can be easily extended to other tube surfaces for which empirical data are available. Advanced tube surfaces are of interest in order to avoid the use of organic additives, unstable at the high temperatures occurring in multiple-effect cycles.

NOMENCLATURE

A	= area (m^2)
c	= concentration (kg/m^3)

C_p	= specific heat (J/kg·K)
D	= diameter (m)
D_{AB}	= diffusion coefficient (m ² /s)
f	= friction coefficient
g	= gravitational acceleration (m/s ²)
h	= convective heat transfer coefficient (W/m ² ·K)
H	= enthalpy (J/kg)
k	= thermal conductivity (W/m·K)
L	= absorber tube length (m)
m	= mass (flow) rate (kg/s)
M	= heat capacity (J/K)
Nu	= $h\delta/k$, Nusselt number
P	= pressure (Pa)
Pr	= ν/α , Prandtl number
Q	= heat rate (W)
r	= tube radius (m)
R	= dampening factor
Re	= vl/ν , Reynolds number ($i = D$, coolant; $l = \delta$, falling film)
Sc	= ν/D_{AB} , Schmidt number
Sh	= $\kappa\delta/D_{AB}$, Sherwood number
t	= time (s)
T	= temperature (K)
U	= overall heat transfer coefficient (W/m ² ·K)
v	= velocity (m/s)
x	= concentration (weight % LiBr)
y	= transverse coordinate (from outer tube wall) (m)
z	= axial coordinate (from top) (m)

Greek Symbols

α	= thermal diffusivity (m ² /s)
$\Gamma = m/2\pi r_o$	= mass flow rate per wetted perimeter (kg/[s·m])
δ	= film thickness (m)
κ	= mass transfer coefficient (m/s)
μ	= dynamic viscosity (N·s/m ²)
ν	= kinematic viscosity (m ² /s)
ρ	= density (kg/m ³)
τ	= characteristic time (s)

Subscripts

c	= coolant
h	= hydraulic
i	= inlet
if	= interface
in	= inner tube wall
ins	= insert
l	= LiBr
max	= maximum
min	= minimum
o	= outer tube wall
s	= solution (bulk)
se	= sensible (heat)

v	= vapor
w	= wall

Superscript

*	= dimensionless quantity
---	--------------------------

REFERENCES

- Andberg, J.W., and G.C. Vliet. 1983. Design guidelines for water-lithium bromide absorbers. *ASHRAE Transactions* 89(1B): 220-232.
- Carnahan, B., H.A. Luther, and J.O. Wilkes. 1969. *Applied numerical methods*, chaps. 2, 6. New York: John Wiley & Sons.
- Close, C.M., and D.K. Frederick. 1978. *Modeling and analysis of dynamic systems*, chap. 8. Boston: Houston Mifflin.
- Cosenza, F., and G.C. Vliet. 1990. Absorption in falling water/LiBr films on horizontal tubes. *ASHRAE Transactions* 96(1): 693-701.
- Davis, P.J., and I. Polonsky. 1970. Numerical interpolation, differentiation and integration. In *Handbook of Mathematical Functions*, 9th printing, M. Abramowitz and I.A. Stegun, eds., pp. 896-897. New York: Dover Publishing, Inc.
- Grossman, G. 1983. Simultaneous heat and mass transfer in film absorption under laminar flow. *Int. J. Heat Mass Transfer* 26(3): 357-371.
- Grossman, G. 1984. Heat and mass transfer in film absorption. In *The Handbook for Heat and Mass Transfer Operations*, N.P. Cheremisinoff, ed. Gulf Pub. Co.
- Hobler, T. 1966. *Mass transfer and absorbers*, pp. 94-95. Warsaw: Wydawnictwa Naukowo-Techniczne.
- Incropera, F.P., and D.P. DeWitt. 1990. *Fundamentals of heat and mass transfer*, 3d ed., chap. 8.
- Kays, W.M., and H.C. Perkins. 1985. Forced convection internal flow in ducts. In *Handbook of Heat Transfer Fundamentals*, 2d ed., W.M. Rohsenow, J.P. Hartnett, and E.N. Ganic, eds., pp. 7.26-7.30. New York: McGraw-Hill.
- Knudsen, J.G. 1973. Heat transmission. In *Chemical Engineers' Handbook*, 5th ed., R.H. Perry and C.H. Chilton, eds., pp. 10-14. New York: McGraw-Hill.
- Le Goff, H., A. Ramadane, and P. Le Goff. 1985. Modélisations des transferts couples de matière et de chaleur dans l'absorption gaz-liquide en film ruisselant laminaire. *Int. J. Heat Mass Transfer* 28(11): 2005-2017.
- McCready, M.J., and T.J. Hanratty. 1984. Concentration fluctuations close to a gas-liquid interface. *AIChE Journal* 30(5): 816-817.
- Patnaik, V., H. Perez-Blanco, and W.A. Miller. 1999. Experimental validation of a simple analytical model for the design of vertical tube absorbers. In progress.
- Perez-Blanco, H. 1988. A model of an ammonia-water falling film absorber. *ASHRAE Transactions* 94(1): 467-483.

- Seban, R.A. 1978. Transport to falling films. *Sixth Int. Heat Transfer Conference*, Toronto, Aug. 7-11, Vol. 6, pp. 417-428. Washington, DC: Hemisphere Pub. Corp.
- Stoecker, W.F., and J.W. Jones. 1982. *Refrigeration and air conditioning*. New York: McGraw-Hill.
- Yih, S.M., and K.Y. Chen. 1982. Gas absorption into wavy and turbulent falling liquid films in a wetted-wall column. *Chem. Eng. Commun.* 17: 123-136.
- Yueksel, M.L., and E.U. Schluender. 1988. Heat and mass transfer in non-isothermal absorption of gases in falling liquid films. *Waerme- und Stoffuebertragung* 22(3-4): 209-217.

APPENDIX

FORMULATION—THE HEAT AND MASS BALANCE

The theoretical model is constructed from two energy balances and a mass balance on an infinitesimally thin slice of the absorber tube, as illustrated in Figure A1. These balances yield three independent equations in the three dependent variables of the problem—coolant temperature, solution (bulk) temperature, and solution mass flow rate—and the independent variable—vertical distance from the top of the absorber tube.

We first consider a control volume of length dz around the falling-film section only. In Figure A1, this is indicated by ABCD. Here, the sum of the heat transferred by conduction through the tube wall to the coolant (dQ_{se}) and the heat convected in and out of ABCD by the solution and vapor must be equal to zero, i.e.,

$$-dQ_{se} + m_s C_{p_s} T_s - (m_s + dm_s) C_{p_s} (T_s + dT_s) + dm_s H_v = 0. \quad (A1)$$

The mass balance on control volume ABCD (coolant mass flow rate stays constant and is hence an operating parameter in the model) yields

$$dm_s = dm_v. \quad (A2)$$

Expressing the incremental mass absorbed in terms of an overall mass transfer coefficient, k_s , gives

$$dm_s = \kappa_s dA_o (c_s - c_{if}). \quad (A3)$$

In control volume EFGH, the sum of the heat conducted through the wall from the solution (dQ_{se}) and the heat convected in and out of EFGH by the coolant must be zero. This yields the third independent equation:

$$dQ_{se} - m_c C_{p_c} T_c + m_c C_{p_c} (T_c + dT_c) = 0. \quad (A4)$$

Equations A1 and A4 are linked by the infinitesimal absorber heat load, dQ_{se} , which can be expressed in the conventional form as the product of an overall heat transfer coefficient that depends on the thermal resistances due to

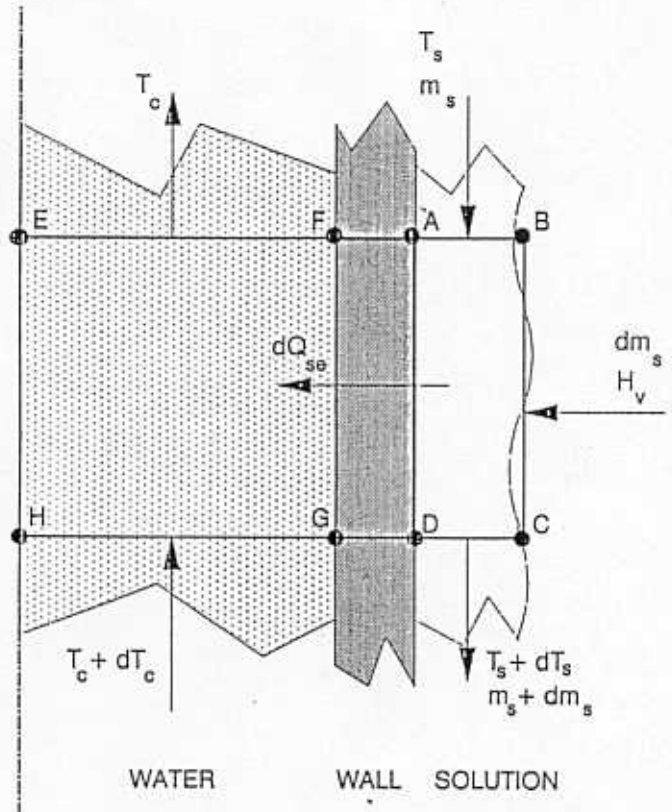


Figure A1 Schematic of the control volumes.

the convective cooling water, the conductive wall and the convective falling film, and the temperature difference. Based on the outer surface area, dA_o , this relation is

$$dQ_{se} = U dA_o (T_s - T_c) \quad (A5)$$

and thus the overall heat transfer coefficient simply characterizes the transport of energy between the falling film and the coolant.

Combining Equations A1 and A4 and integrating from the top of the tube to the value of z for the control volume in order to factor in the absorber (solution) inlet conditions, we obtain

$$H_v (m_s - m_{s_i}) + m_c C_{p_c} (T_c - T_{c_i}) - C_{p_s} (m_s T_s - m_{s_i} T_{s_i}) = 0. \quad (A6)$$

Substitution of this equation into Equation A5, through the variable T_c , yields the first of the three first-order ordinary differential equations for the three dependent variables. The remaining two ODEs result from the combination of Equations A2 and A3 and Equations A4 and A5, respectively. Nondimensionalizing with respect to the coolant outlet properties and the total (outer) surface area of the tube, the equations take the following final forms:

$$\frac{dT_s^*}{dz^*} = \frac{1}{M_s^*} \left[\frac{dm_s^*}{dz^*} (H_v^* - C_{p_s}^* T_s^*) + U^* (1 - T_s^* (1 - M_s^*) - H_v^* (m_s^* - m_{s_i}^*) - M_{s_i}^* T_{s_i}^*) \right] \quad (A7)$$

where dm_s^*/dz^* is obtained from manipulating Equation A3 to yield the second ODE:

$$\frac{dm_s^*}{dz^*} = \frac{2\pi r_o L}{m_c} \cdot \frac{Sh D_{AB}}{\delta} \cdot \rho_s (x_s - x_{if}) \quad (A8)$$

where the film thickness,

$$\delta = \left(\frac{3 \cdot \mu \cdot \Gamma}{\rho^2 \cdot g} \right)^{\frac{1}{3}} \quad (A9)$$

and the velocity distribution are obtained from Nusselt's classic solution to the hydrodynamic problem (Patnaik et al. 1992). For the coolant temperature, we have the third ODE:

$$\frac{dT_c^*}{dz^*} = -U^* (T_s^* - T_c^*) \quad (A10)$$

Assuming a linear temperature profile across the film thickness, the interfacial gradient of the temperature in the transverse direction can be easily approximated by deriving an expression for the "location" of the bulk solution (mixing-cup) temperature. With heat conduction into the film thus approximated in the energy balance at the interface (Figure A2), we find a relation between the interface temperature, the bulk solution temperature, and the local axial gradient of the mass absorbed (Equation 5).

The Dampening Factor

In analogy with first-order step-response theory in electrical measurements, the dampening factor is an

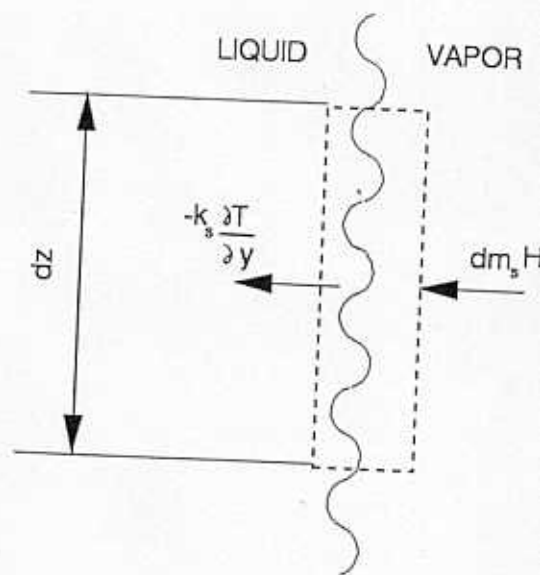


Figure A2 Energy balance at the interface.

increasing function of time (asymptotically approaching unity) that has the form:

$$R = 1 - e^{-t/\tau} \quad (A11)$$

where the characteristic (response) time can be shown to

$$\tau = \left(\frac{\delta}{A k_s} \right) \cdot (\rho_s \delta A \cdot C_{p_s}) \quad (A12)$$

by establishing an analogy between electrical capacitance and resistance and thermal capacity and resistivity, respectively, or,

$$\tau = \frac{\delta^2}{\alpha_s} \quad (A13)$$

Replacing the time variable with z/v_{max} , we finally obtain the dampening factor:

$$R = 1 - e^{-\frac{z \alpha_s}{v_{max} \delta^2}} \quad (A14)$$